Seismic, Geotechnical, and Earthquake Engineering Site Characterization

Oz Yilmaz and Murat Eser, Anatolian Geophysical, Istanbul, Turkey, and*
Mehmet Berilgen, Yildiz Technical University, Istanbul, Turkey

Summary

We determined the seismic model of the soil column within a residential project site in Istanbul, Turkey. Specifically, we conducted refraction seismic survey at 20 locations and estimated the P- and S-wave velocity-depth profiles down to a depth of 30 m. We then combined the seismic velocities with the geotechnical borehole information regarding the lithology of the soil column and determined the site-specific geotechnical earnthquake engineering parameters for the site. Specifically, we computed the maximum soil amplification ratio, maximum surface-bedrock acceleration ratio, depth interval of significant acceleration, maximum soil-rock response ratio, and design spectrum periods T_A-T_B.

Introduction

Figure 1 shows the location map of the site. The size of the area is approximately 40 acres. Elevations vary between 125-180 m. Topography is fairly flat in the western half of the site while there is a downhill slope in the northerly direction in the eastern half. The top soil is entirely clay. The site has been designated for a residential project that involves construction of multistorey apartment blocks.

Figure 1. Location map for the seismic survey conducted within the residential development project site. The survey cocnsists of refraction profiling at 20 locations.

Data Acquisition

At each of the 20 locations (KS01-KS20) within the project site (Figure 1), we deployed a receiver spread with 48 4.5-Hz vertical geophones at 2-m intervals. We used a buffalo gun at the bottom of a charge hole with a diameter of 10-cm and a depth of 30-cm and acquired three shot records with source locations at each end of the spread and at the center of the spread (Figure 2). The sampling rate for recording is 0.5 ms and the record length is 2 s. The orientation of the receiver spread at each location was chosen such that the elevation change along the receiver spread is minimal.

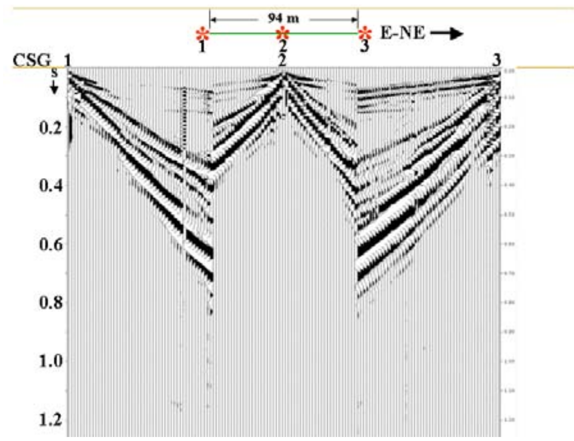

Figure 2. Example common-shot gathers (CSG) acquired by a 94-m receiver spread (the green bar on top). The red asterisks denote the shot locations --- two shots with 2-m offset from the ends of the receiver spread and a shot at the center of the spread.

Data Analysis

By applying a nonlinear traveltime tomography (Zhang and Toksoz, 1998) to the first-arrival times picked from the three shot records, we estimated a near-surface P-wave velocity-depth model along the receiver spread at each of the 20 locations. By applying smoothing during the inversion and lateral averaging after the inversion, we then obtained a P-wave velocity-depth profile down to a depth of 30 m representative of each location.

Next, we identified the off-end shot record with the most pronounced dispersive surface-wave pattern and performed plane-wave decomposition to transform the data from offset-time to phase-velocity versus frequency domain. A dispersion curve associated with the fundamental mode of Rayleigh-type surface waves was picked in the transform domain based on the maximum-energy criterion and inverted to estimate the S-wave velocity as a function of depth as shown in Figure 3 (Park et al., 1999; Xia et al., 1999).

Following the analysis of refracted waves to estimate the P-wave velocities and the analysis of surface waves to estimate the S-wave velocities at each of the 20 locations, we correlated the velocities and generated velocity contour maps for depth levels 0-30 m at 4-m intervals (Figures 3). Additionally, we computed the ratio of the P-wave velocities to the S-wave velocities as a function of depth and generated the velocity-ratio contour maps. Based on the velocity variations, the site was divided into three sections --- the western section with relatively low S-wave velocities, the eastern section with relatively high S-wave velocities and the transitional central section. We then drilled geotechnical boreholes within each section down to a depth of 50 m at locations coincident with the center of the spreads KS05, KS10, and KS14.

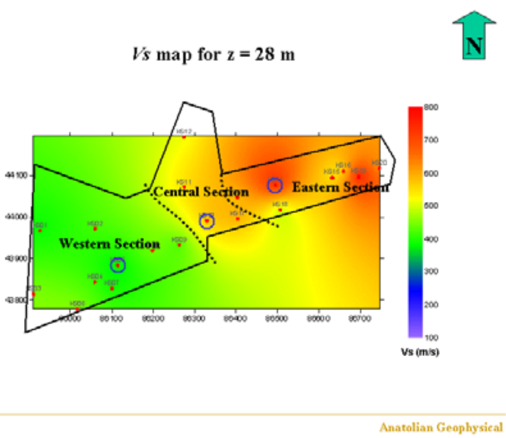

Figure 3. The S-wave velocity map for a depth level of 28 m. The red dots represent the spread centers at the 20 locations where the seismic survey was conducted. The blue circles denote the geotechnical borehole locations for each of the three sections.

Estimation of Geotechnical Earthquake Engineering Parameters

For each section within the project site (western, central, and eastern), the S-wave velocities within the soil column combined with the borehole lithology (Figure 4) were used to determine the geotechnical earthquake engineering parameters. We begin with a rock-site SH accelerogram that describes the time history of the strong ground motion associated with the August 1999 Izmit earthquake (Yilmaz et al., 2005). Given the S-wave velocity-depth profile, the geotechnical borehole information, and the accelerogram that describes the ground motion at the rock site, we calculated the accelerogram that simulates the ground motion at the soil site (Figure 5) for each of the three sections within the site. This one-dimensional site-response analysis was performed using a frequency-domain algorithm that models the nonlinear material behavior of the soil column as an equivalent linear system (Bardet et al., 2000).

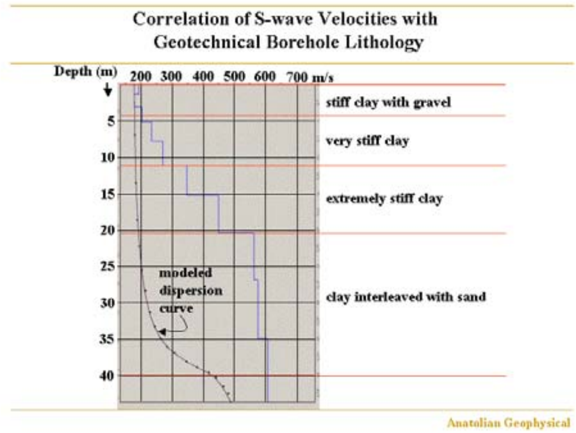

Figure 4. Correlation of the S-wave velocities with the lithology column from the geotechnical borehole at the center of the spread at location KS10 (central section).

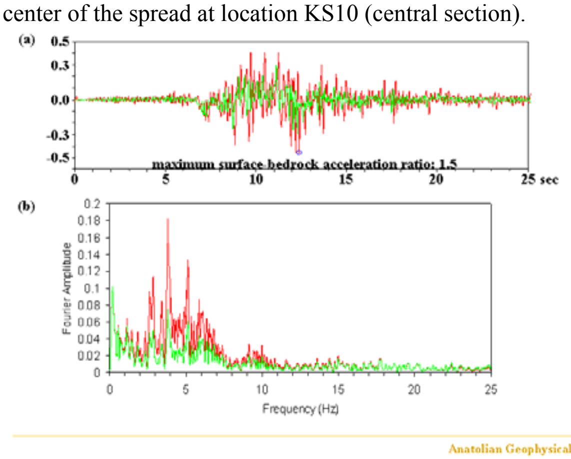

Figure 5. Analysis for geotechnical earthquake engineering parameters at site KS10 (central section): (a) The accelerogram that describes the bedrock motion associated with the August 1999 Izmit earthquake measured at the rock site (green), which is assumed to be equivalent to the response at the soil-bedrock interface at the soil site (upscaled to a maximum acceleration value of 0.3g), and the accelerogram that describes the ground motion at the soil site KS10 within the western section (red) modeled by using the velocity and borehole information given by Figure 4. The maximum surface-bedrock acceleration ratio is 1.5. (b) The amplitude spectra of the measured and modeled accelerograms. Note that the significant amplification within soil column occurs between 0-12 Hz bandwidth.

In earthquake engineering, the soil response to an earthquake motion is calculated based on the scenario that corresponds to a maximum possible peak ground acceleration that may occur at a location (Kramer, 1996). Hence, the accelerogram at the rock site (equivalently, at the soil-bedrock interface), was actually upscaled to a maximum value of 0.3g before the modeling of the accelerogram at the soil sites within each section (KS05, KS10, and KS14).

From Figure 5, we determined for each section the ratio of the maximum ground acceleration at the soil site to the maximum acceleration at the soil-bedrock interface --- often referred to as *maximum surface-bedrock acceleration ratio.* For each section, we also computed the maximum acceleration as a function of depth, and determined the depth range for which surface-bedrock acceleration ratio is significant (Figure 6a). Specifically, as the bedrock motion is upward propagated through the soil column, maximum acceleration values are computed at discrete depth levels through the soil column. From Figure 6b, we determined the peak spectral amplitude at the soil site and the frequency at which this peak occurs (3.3 Hz). The latter is called the natural frequency of the soil column and the period that corresponds to the peak-amplitude frequency is called the *natural period* of the soil column (0.3 s). Also from Figure 6b, we computed the ratio of the peak spectral amplitude at the soil site to the spectral amplitude corresponding to the same frequency at the rock site (2.9). This is called the *maximum soil amplification ratio*, which is a measure of how much the soil column amplifies the earthquake motion that occurs at the soil-bedrock interface.

Next, for each section within the site, we computed the response spectra (Figure 6c) which describe the response of structures (buildings) with a range of natural periods to the modeled ground motion at the soil site and the actual ground motion at the rock site. The structure is defined as a spring system with a single degree of freedom (SDOF), usually with damping ratio of 5%. From Figure 6c, we determined the maxima of the response spectra at the ground level (8g) and soil-bedrock interface (3g), and computed *the maximum soil-rock response as the spectral acceleration ratio* (2.4). We also determined *the design spectrum periods T_A-T_B* (0.05-0.55 sec). T_A and T_B correspond to the minimum and maximum periods for which the spectrum is nearly flat. Outside the T_A-T_B bandwidth, the spectrum ramps down rapidly.

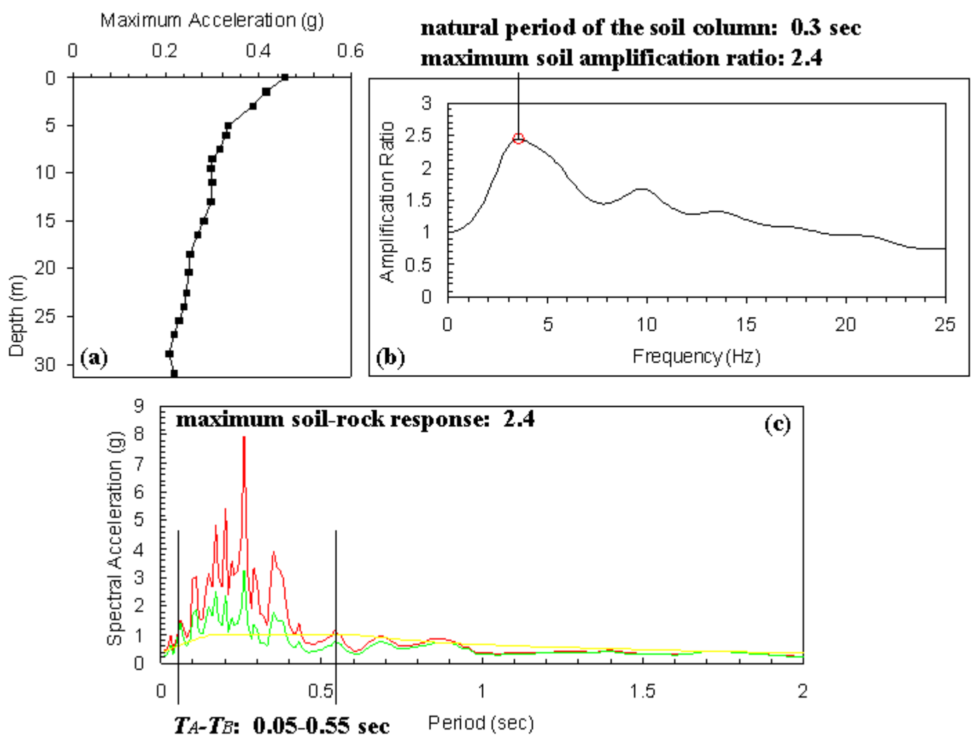

Figure 6. Analysis for geotechnical earthquake engineering parameters at site KS10 (central section): (a) Maximum acceleration as a function of depth, (b) soil-bedrock amplification ratio, and (c) site-specific design spectra for the rock site (green) and the soil site (red), and the code-speicifc design spectrum for the soil site (yellow). Note that the most significant acceleration values at the rock site occurs between T_A-T_B: 0.05 – 0.55 sec.

Table 1. Geotechnical earthquake engineering parameters.

Section	*Maximum soil amplification ratio*	*Nautral period of the soil column (sec)*	*Maximum surface-bedrock acceleration ratio*	*Depth interval with significant acceleration (m)*	*Maximum soil-rock response*	*Design spectrum periods TA – TB (san)*
Western	2.2	0.4	1.3	0 - 10	1.3	0.05 - 0.60
Central	2.4	0.3	1.5	0 - 15	2.4	0.05 - 0.55
Eastern	2.8	0.15	1.7	0 - 10	2.1	0.05 - 0.65

Conclusions

Site investigations require multidisciplinary investigation by the geologist, seismologist, geotechnical and earthquake engineers. Listed in Table 1 are the geotechnical earthquake engineering parameters for each of the three section within the site. Combined with the parameters for the soil dynamics, such as the bearing capacity, these parameters are used by the geotechnical engineer for soil classification and by the civil engineer for structural design of buildings.

Acknowledgements

We thank the Hanyapi Real Estate Development Corp., Istanbul, for giving us the opportunity to conduct this integrated seismic project and granting the permission for publishing the results.

References

Bardet J., Ichii, K., and Lin C., 2000, Manual of EERA: a computer program for equivalent-linear earthquake site response analysis of layered soil deposits, University of Southern California.

Kramer, S. L., 1996, Geotechnical Earthquake Engineering, p. 273, Prentice-Hall, New Jersey.

Park, C. B., Miller, R. D., and Xia, J., 1999, Multichannel analysis of surface waves: Geophysics, 64, 800-808.

Xia, J., Miller, R. D., and Park, C. B., 1999, Estimation of near-surface shear-wave velocity by inversion of Rayleigh waves: Geophysics, 64, 691-700.

Yilmaz, O., Eser, M., and Berilgen, M., 2006, A case study for seismic zonation in municipal areas, The Leading Edge, March issue, 319-330.

Zhang, J. and Toksoz, M. N., 1998, Nonlinear refraction traveltime tomography: Geophysics, 63, 1726-1737.

EDITED REFERENCES

Note: This reference list is a copy-edited version of the reference list submitted by the author. Reference lists for the 2006 SEG Technical Program Expanded Abstracts have been copy edited so that references provided with the online metadata for each paper will achieve a high degree of linking to cited sources that appear on the Web.

REFERENCES

Bardet, J., K. Ichii, and C. Lin, 2000, Manual of EERA: a computer program for equivalent-linear earthquake site response analysis of layered soil deposits: University of Southern California.

Kramer, S. L., 1996, Geotechnical Earthquake Engineering: Prentice-Hall, Inc., 273.

Park, C. B., R. D. Miller, and J. Xia, 1999, Multichannel analysis of surface waves: Geophysics, **64**, 800–808.

Xia, J., R. D. Miller, and C. B. Park, 1999, Estimation of near-surface shear-wave velocity by inversion of Rayleigh waves: Geophysics, **64**, 691–700.

Yilmaz, O., M. Eser, and M. Berilgen, 2006, A case study for seismic zonation in municipal areas: 75th Annual International Meeting, SEG, Expanded Abstracts, 1105–1108.

Zhang, J., and M. N. Toksoz, 1998, Nonlinear refraction traveltime tomography: Geophysics, **63**, 1726–1737.